Paleoceanography and Paleoclimatology

Supporting Information for

Persistent provenance of South Asian Monsoon induced silicate weathering over the past 27 million years

Sajid Ali[1,2]*, Ed C. Hathorne[1]*, Martin Frank[1]

1GEOMAR Helmholtz Centre for Ocean Research Kiel, D-24148 Kiel, Germany.

2 Birbal Sahni Institute of Palaeosciences (BSIP), 53 University Road, Lucknow-226007, India

Contents of this file

Additional Supporting Information (Files uploaded separately)

Introduction

Here we provide further methodological details concerning the sample pre-treatment, the age model and grain size analyses, as well as further comparison with literature data. The tables present the data compiled from the literature used for comparison of sources as well as the age datums and depth offsets used.

Text S1. Clay minerals and pretreatment with hydroxylamine hydrochloride (HH):

A multitude of pre-treatment methods have been employed before clay mineral and radiogenic isotope analysis of marine sediments (e.g. interlaboratory comparison of Ottner et al.. 2000). Many studies focusing on clay mineralogy treat samples only with H2O2 to remove organic matter before separating the clays (e.g. Lee et al.. 2020) or H2O2 followed by sodium hexametaphosphate solution to disaggregate before separating the < 2 micron fraction. with a further treatment with 0.5M HCl to remove fine carbonates from carbonate rich sediments (e.g. Phillips et al.. 2014). The comparison of splits with or without the 0.5M HCl treatment demonstrated the removal of fine carbonates resulted in stronger XRD peak intensities for the clay minerals (Phillips et al., 2014). On the other hand. studies focusing on the geochemistry and isotope composition of the clays have also employed reductive leaching to remove Fe and Mn oxides before analysis (e.g. Simon et al., 2020). To examine the effect of reductive leaching on clay minerals, Helios Rybicka & Calmano (1988) subjected different clay samples to various

reductive reagents and then measured the exchange capacity and surface area of the clays as well as the elements released by leaching. The hydroxylamine hydrochloride (HH) leach they employed released exchangeable cations and potentially dissolved some of the clays or associated amorphous silicates. The change in the physical properties (specific surface area and exchange capacity) of the clays following the HH leach was modest for kaolinite while no change was detected for the smectite illite mix. For the illite sample the specific surface area remained unchanged and only a small change in exchange capacity of the illite was observed (Helios Rybicka & Calmano 1988). Experiments with combined acetic acid and HH leach solution have shown some dissolution of clay minerals but this is relatively minor (<6% at room temperature for 4 hours) and was found to dissolve more illite and the smectite montmorillonite compared to kaolinte and chlorite (Chester & Hughes 1967). These authors further suggested the structure of the clay minerals remained in tact as the amounts of Fe and Mn released by the combined acid-reducing solution were comparable to that expected in non-lattice positions. The clay mineral data like those generated here must be considered semi-quantitative (e.g. Hiller 1999) meaning only relative changes should be interpreted. Although the various pre-treatment techniques applied before analysis must have contributed to the large range of clay mineral % data reported by an inter-laboratory study of two natural samples. a specific affect of acid treatment on chlorite was not detectable and a large range of values was obtained applying different evaluation techniques to the same diffractograms (Ottner et al. 2000). Considering such inconsistencies the agreement between clay mineral data generated from neighbouring drill cores in the Andaman Sea using different pretreatments is good (Supplementary Table 1) and provides confidence in the clay mineral data of this study that were generated with the same technique and conditions..

	smectite	illite	kaolinite	chlorite	sm/il+chl
Average 0-2 Ma Ali et al. (unpublished)	38.0	37.6	15.9	8.6	0.9
Average 0-2 Ma Lee et al. (2020)	34.2	36.5	15.6	13.7	0.7
Average 0-2 Ma Phillips et al. (2014)	43.0	28.8	13.1	15.1	1.0
Average 6-8 Ma Ali et al. (unpublished)	53.9	27.5	13.9	4.7	1.7
Average 6-8 Ma Lee et al. (2020)	57.9	23.3	11.1	7.7	1.9
Average 6-8 Ma Phillips et al. (2014)	49.0	26.1	16.1	8.8	1.4

Table S1. Comparison of clay mineral abundance data for NGHP Site 17 from Phillips et al. (2014) following H2O2 and 0.5M HCl decarbonation pre-treatment and from neighbouring IODP Site U1447 from Lee et al. (2020) following H2O2 pre-treatment only with unpublished data for NGHP Site 17 prepared and measured with the same technique used here.

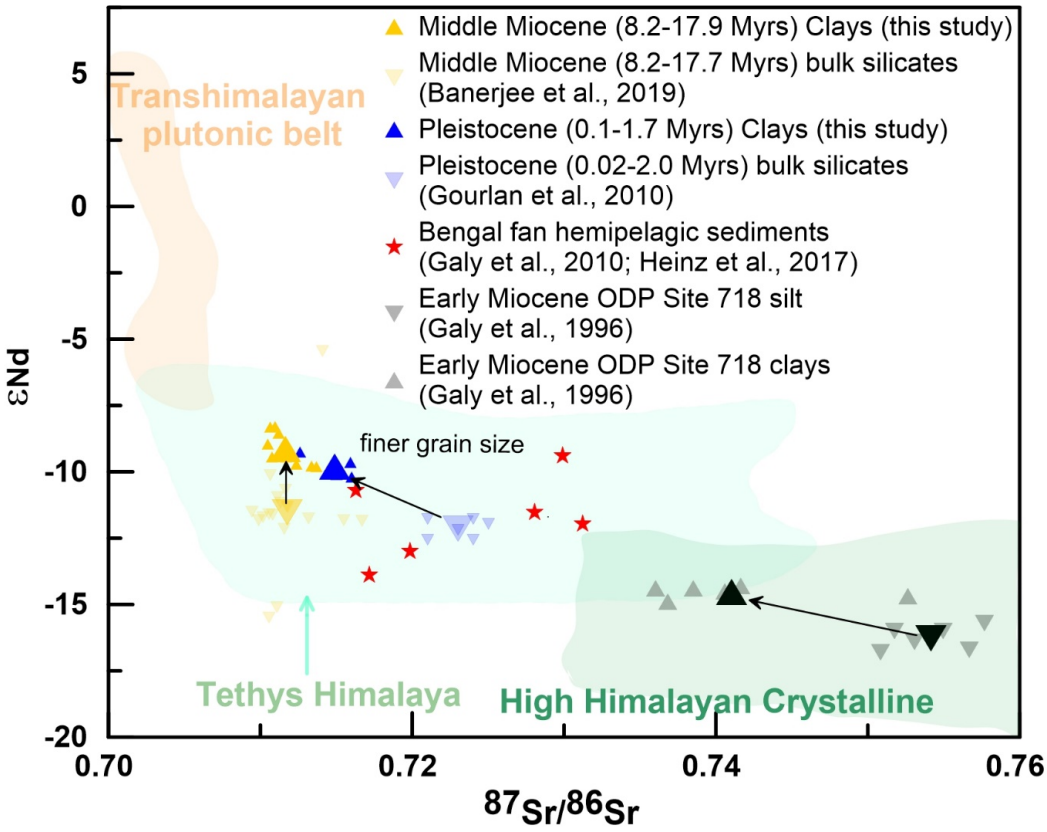

Figure S1. Nd-Sr isotope compositions of the clay size fraction compared with literature data for bulk silicate sediments of similar age from the same site (ODP Site 758), clay and silt sized sediments from early Miocene samples from the distal Bengal fan (ODP Site 718) and Bengal fan hemipelagic sediments. The average values for an age range are shown by larger symbols and lines join the clay and bulk (or silt) values of similar age. The fields for 3 major Himalayan rock formations are after Gourlan et al. (2010) and references therein.

Text S2. Age Model:

The meter scale correlation of ODP Site 758A cores to the IODP Site U1443 spliced image is shown in Supplementary Fig. 3. No finer correlation by stretching the cores has been attempted. Aligning the cores was straight forward for the upper 150 m where clear cycles and variations in sediment colour exist. Below this the sediment colour became monotonous making precise correlation difficult but as the offsets between cores are cumulative the possible errors are small compared to the million year resolution of the ODP Site 758 records. Having placed the ODP Site 758A cores on the same depth scale as the U1443 splice we use the biostratigraphic age data from the expedition report (Clemens et al.. 2016) to generate an age model (Supplementary Data 2, Fig. 4). The shipboard paleomagnetic data are used until the middle Miocene where the stratigraphy is based on high resolution benthic foraminifera oxygen and carbon isotopes (Lübbers et al.. 2019). The high resolution benthic foraminifera stable isotope data reveal there was a slow but continuous sedimentation through this important interval of our record with the pronounced changes in clay mineralogy. The U1443 stable isotope record has been

tuned to a higher sedimentation rate reference record from the South China Sea and the stratigraphy is supported by improved shore based biostratigraphic and paleomagnetic work (Lübbers et al., 2019). Below the middle Miocene the age model is based on biostratigraphic derived linear sedimentation rates but these are consistent with rates derived from unpublished high resolution benthic foraminifera stable isotopes until 17.7 Myrs ago (K. Kochhran. personal communication) and preliminary shore based paleomagnetic data for the earliest Miocene (Y. Usui. personal communication). The original ODP Site 758 age constraints (Dehn et al., 1991; Pierce et al., 1989) have been updated to the more recent GTS12 time scale (Gradstein and Ogg, 2012) and overlap with those from Site U1443 on the composite depth scale. (Supplementary Data 2).

Figure S2. Comparison of the clay smectite (%) content with the 87Sr/86Sr of the clays and the difference between the clay 87Sr/86Sr and the contemporaneous (depositional age) 87Sr/86Sr of global seawater (McArthur et al.. 2001).

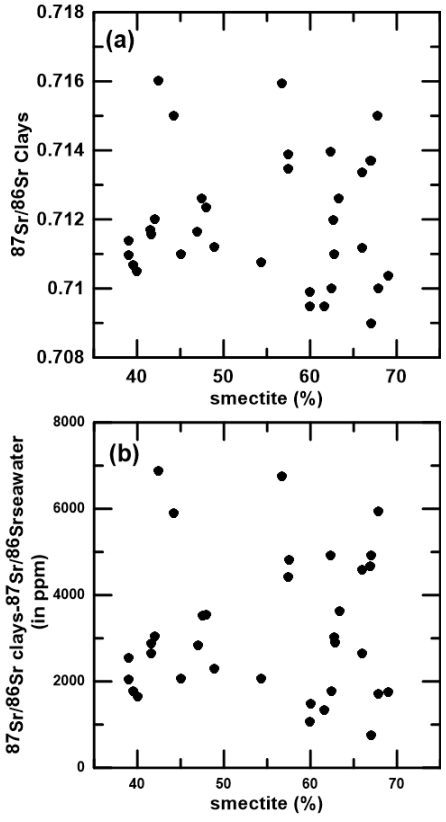

Figure S3a. Colour line scanning image composite overview of the upper 220 meters of the IODP Site U1443 Splice (S) composed of holes U1443A, B, C, and D, with gamma ray attenuation (GRA) data plotted on top (the colour of the line being a function of core number). The core numbers are labelled and the yellow and red lines indicate splice tie points where the splice changes hole. ODP Site 758A core images have been cropped and compiled and offset to visually align with the colour variations of the U1443 splice. Core offsets derived in this way are given in Data Set S3. This figure was made using Igor Pro software and macros detailed in Wilkens et al. (2017).

Figure S3b. As in supplementary fig. 3a but for the upper 50 meters of the IODP Site U1443 Splice (S).

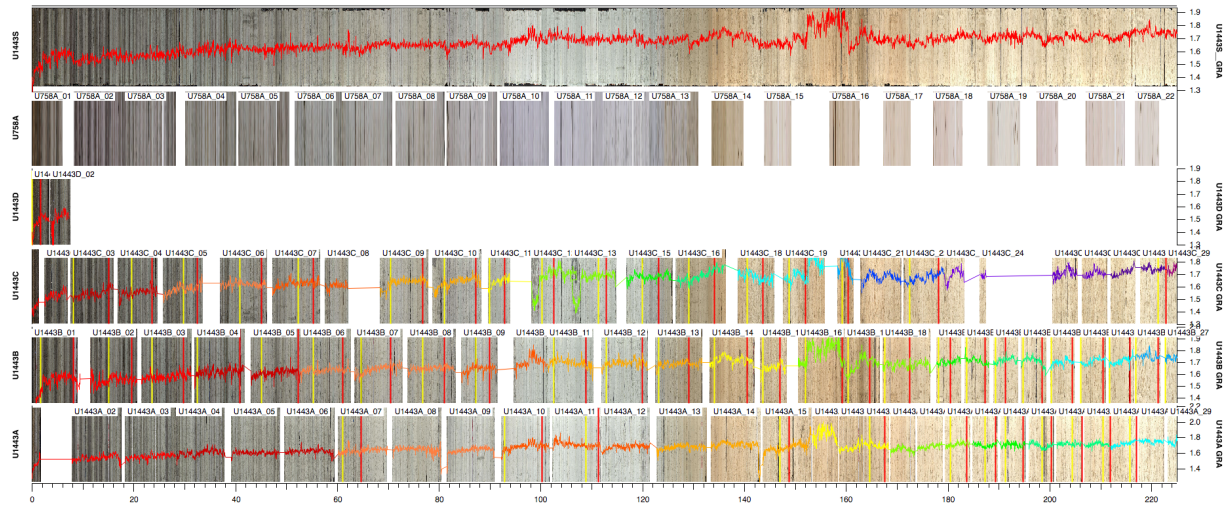

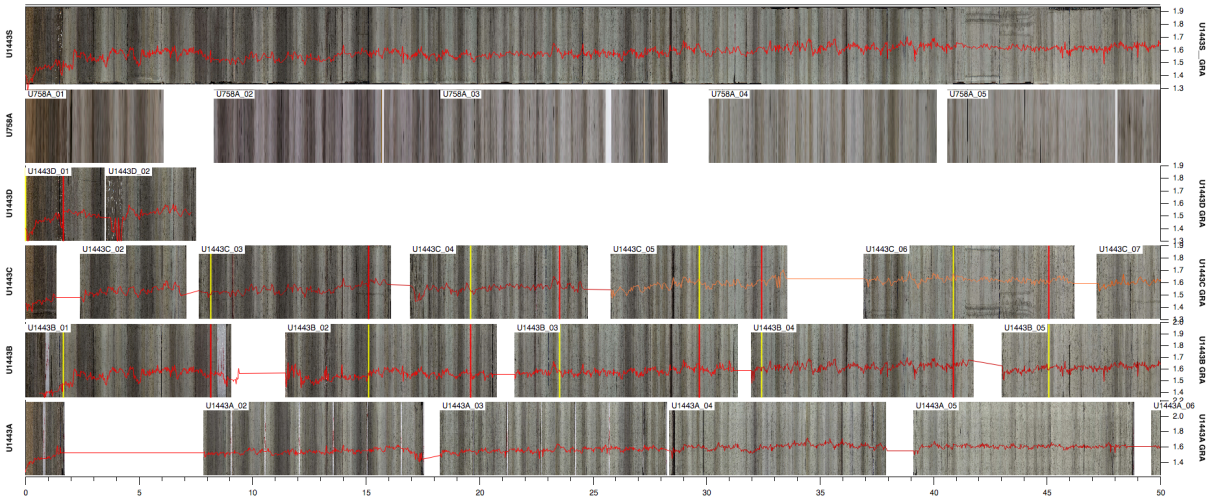

Figure S3c. As in supplementary fig. 3a but for the 50 - 100 meter interval of the IODP Site U1443 Splice.

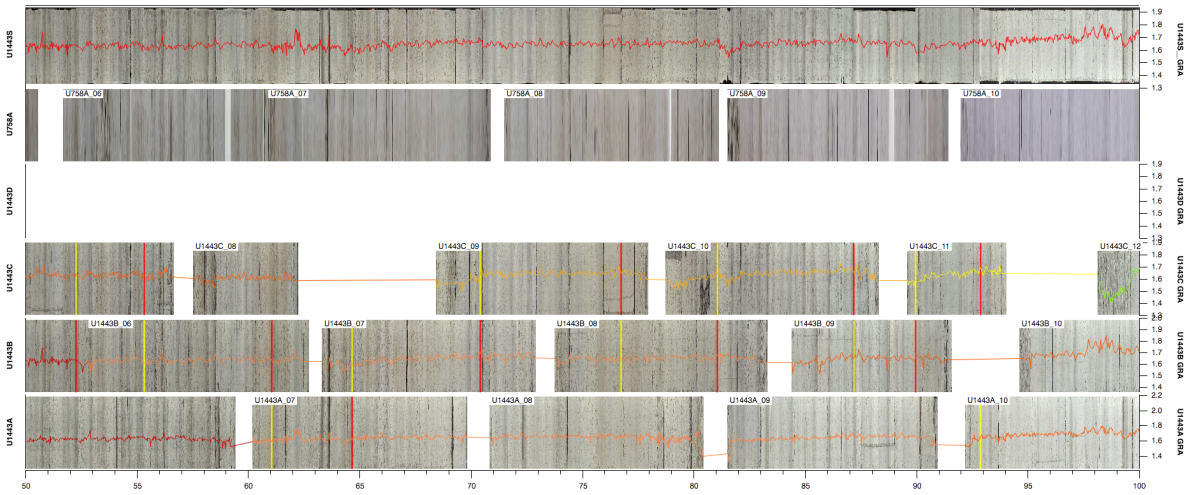

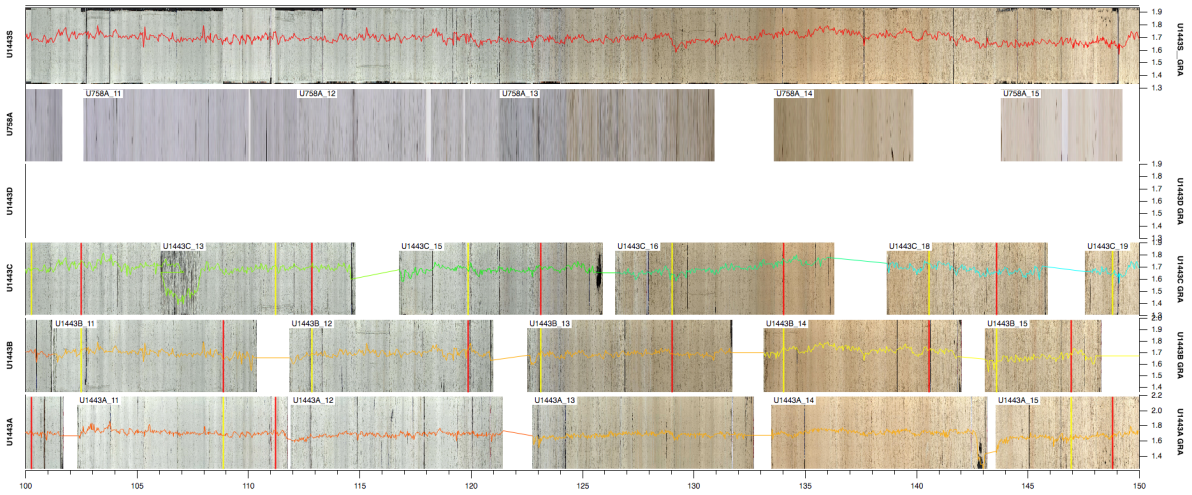

Figure S3d. As in supplementary fig. 3a but for the 100 - 150 meter interval of the IODP Site U1443 Splice.

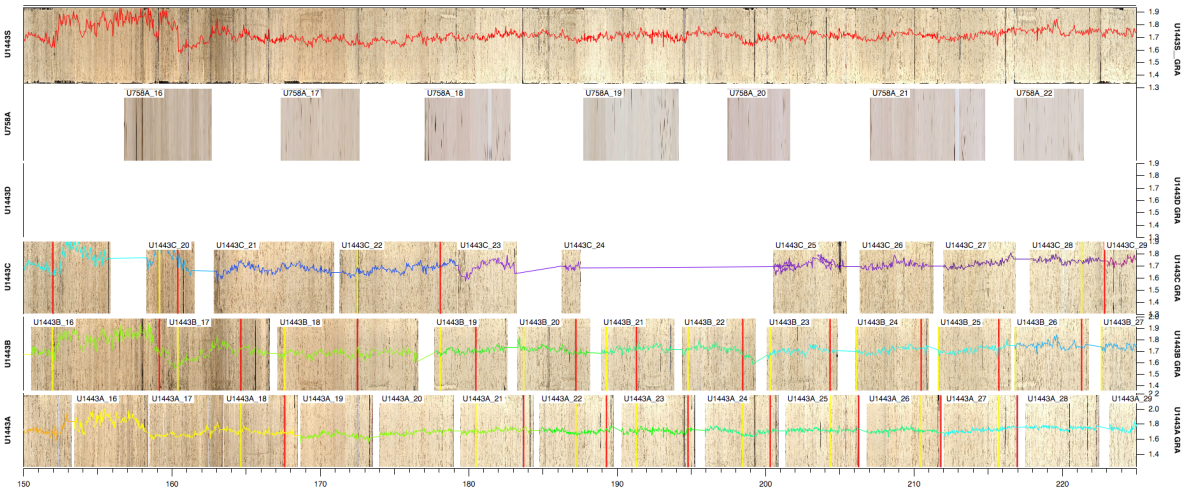

Figure S3e. As in supplementary fig. 3a but for the 150 - 220 meter interval of the IODP Site U1443 Splice.

Figure S4. Age model of the IODP Site U1443 Splice used to determine the ages of the samples from ODP Site 758 in this study. For the first 9 Myrs (red section) a linear sedimentation rate of 14.16 m/Myr is obtained using biostratigraphic and paleomagnetic data from Clemens et al. (2016) Below this (green section) the high resolution benthic foraminifera stable isotope stratigraphy with updated biostratigraphic and paleomagnetic data from Lübbers et al. (2019) is used. Like Lübbers et al. (2019) we utilise linear interpolation between the stable isotope ties points and below those a linear sedimentation rate of 3.81 m/Myr using biostratigraphic data from Clemens et al. (2016). For the early Miocene and Oligocene (orange section) only biostratigraphic data from Clemens et al. (2016) are used but preliminary shore based paleomagnetic results support the inferred sedimentation rate of 7.40 m/Myr.

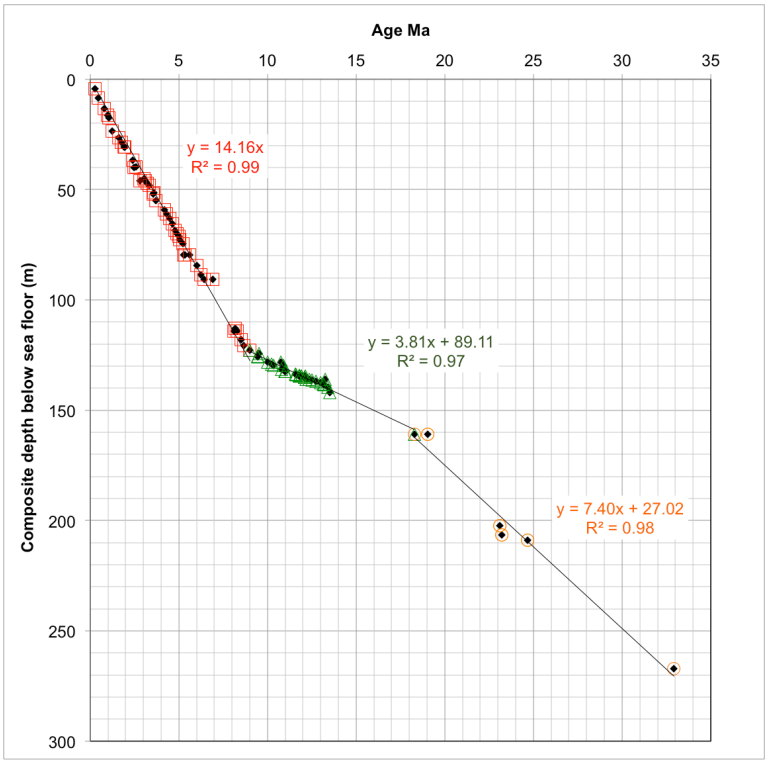

Text S3. Laser grain-size analyses:

Prior to grain size analyses sediment samples were treated with 0.5 N Hydrochloric acid (HCl) and 10% hydrogen peroxide to remove carbonate fractions and organic material, respectively. The mixture was then rinsed several times with de-ionized water prior to measurements and gently shaken to achieve disaggregation. The suspension was then poured into the fluid module of the particle size analyzer. Ultrasonic oscillation was avoided during measurement as suggested by Trentesaux et al. (2001) and followed by Jouissain et al. (2016) to get rid of any break of brittle minerals e.g. Micas. The grain size distributions were determined using a laser diffraction particle size analyzer Beckman Coulter LS I3 320 at the Institute of Geosciences. University of Kiel. Germany. yielding 116 size classes from 0.04 to 1908 μm. The grain size of detrital fraction of ODP Site 758 ranges from 0.4 μm to 390 μm. The results were processed using the freely available gradistat8.0 software for sediment parameters (Blott and Pye. 2001). The relative distribution of sand (>63 μm to 2 mm). silt (63 to 2 μm) and clay (<2 μm). is given in Supplementary Fig. 5 that ranges from 1.4 to 38.7 % (average 11.9 %). 56.5 to 90.9 % (average 76.8 %). 3.1 to 24.9 % (average 11.3 %). respectively. The mean grain-size varies from 8.9 μm to 59.2 μm (average 25.8 μm) and median values range from 4.4 to 47.6 (average 16.4 μm) (Supplementary Fig. 6).

Figure S5. Grain size distribution of detrital bulk silicate fractions of ODP Site 758.

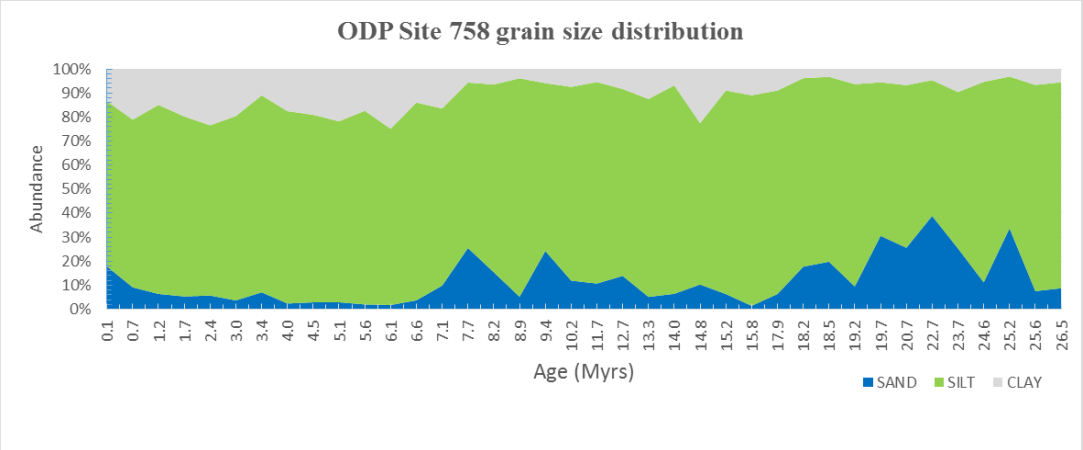

Figure S6. Median and mean grain size of bulk silicate fractions of ODP Site 758 sediments compared with the mineral flux (Hovan and Rea. 1992) recalculated using the new sedimentation rates from the revised age model.

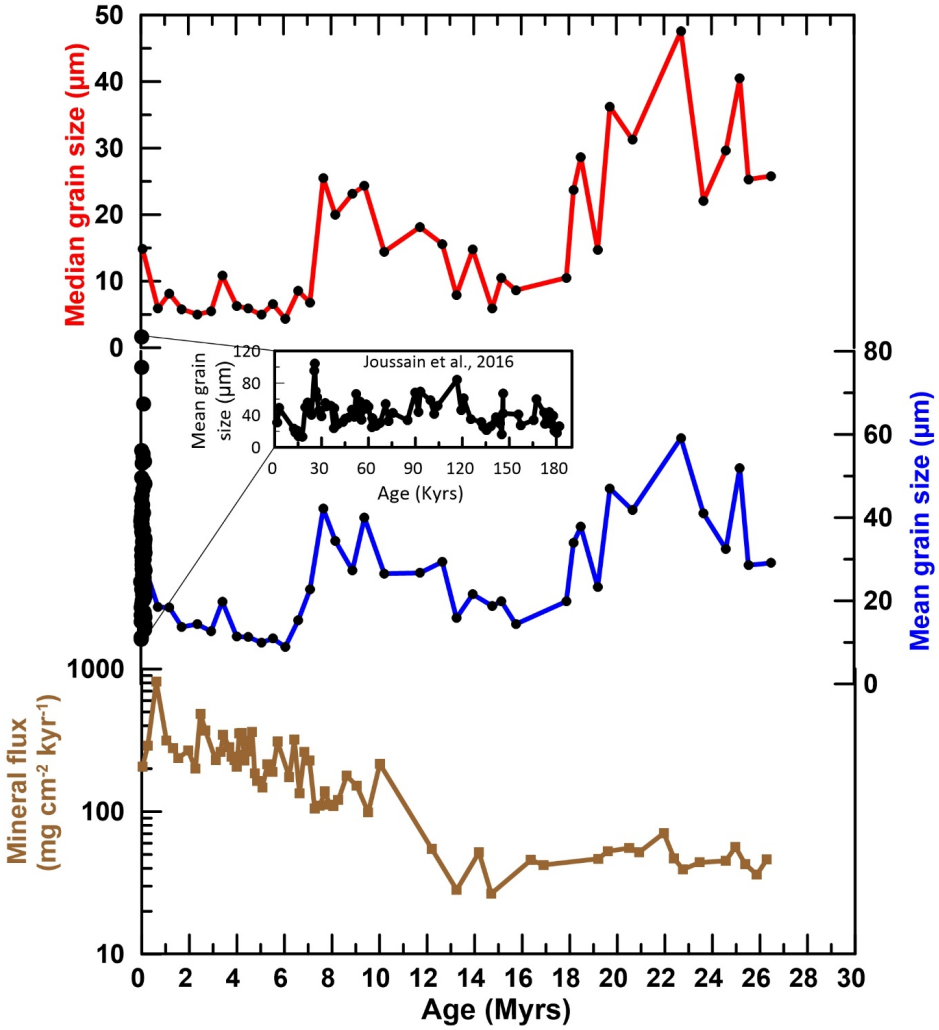

Data Set S1. Radiogenic Sr, Nd and Pb isotope data and clay mineral abundances of the < 2 μm size fraction of ODP Site 758A.

Data Set S2. Age datums used for the age model from Clemens et al. (2016) and Lübbers et al. (2019)

Data Set S3. Depth offsets to place ODP Site 758A hole CSF onto U1443 composite depth CCSF-A

Data Set S4. Compiled Sr, Nd and Pb isotope values from the literature. References are given with the main article.